Geomechanics and Engineering, *Vol. 32, No. 3 (2023) 245-254*
https://doi.org/10.12989/gae.2023.32.3.245

Stability analysis of settled goaf with two-layer coal seams under building load-A case study in China

Yao Lu[1], Ning Jiang*[1], Changxiang Wang[2], Meng Zhang[2], Dezhi Kong[3] and Haiyang Pan[1,4]

[1]*State Key Laboratory of Mining Disaster Prevention and Control Co-Founded by Shandong Province and the Ministry of Science and Technology, Shandong University of Science and Technology, Qingdao 266590, China*
[2]*College of Safety Science and Engineering, Anhui University of Science and Technology, Huainan 232000, China*
[3]*Wenzhou Medical University, Wenzhou 325000, China*
[4]*General Institute of Exploration and Research of China National Administration of Coal Geology, Beijing 10039, China*

(*Received June 22, 2022, Revised January 8, 2023, Accepted January 12, 2023*)

Abstract. Through qualitative analysis and quantitative analysis, the contradictory conclusions about the stability of the settled goaf with two-layer coal seams subject to building load were obtained. Therefore, it is necessary to combine the additional stress method and numerical simulation to further analyze the foundation stability. Through borehole analysis and empirical formula analogy, the height of water-conducting fracture zone in No.4 coal and No.9 coal were obtained, providing the calculation range of water-conducting fracture zone for numerical simulation. To ensure the accuracy of the elastic modulus of broken gangue, the stress-strain curve were obtained by broken gangue compression test in dried state of No.4 coal seam and in soaking state of No.9 coal seam. To ensure the rationality of the numerical simulation results, the actual measured subsidence data were retrieved by numerical simulation. FISH language was used to analyze the maximum building load on the surface and determine the influence depth of building load on the foundation. The critical building load was 0.16 MPa of No.4 settled goaf and was 1.6 MPa of No.9 settled goaf. The additional stress affected the water-conducting fracture zone obviously, resulted in the subsidence of water-conducting fracture zone was greater than that of bending subsidence zone. In this paper, the additional stress method was analyzed by numerical simulation method, which can provide a new analysis method for the treatment and utilization of the settled goaf.

Keywords: ad-ditional stress method; building loads; crushing gangue compression test; foundation stability; settled goaf with two-layer coal seams

1. Introduction

After the formation of the coal goaf, the overlying rock structure in goaf is easily affected by the building loads above the goaf, resulting in the secondary disturbance of the roof rock (Karabork *et al.* 2014, Pan *et al.* 2022, Tan *et al.* 2022, Jiang *et al.* 2020). However with the accelerated urbanization and industrialization in China and the increasing density of infrastructure construction, many goafs of coal mines are gradually classified as industrial, commercial and transportation land (Soomro *et al.* 2022, Toprak *et al.* 2021, Tan *et al.* 2021, Wang *et al.* 2019, Yao *et al.* 2022, Jiang *et al.* 2021). Therefore, it is of great theoretical and practical significance to study the stability of building foundation above settled goafs.

The mining regulation stipulates that, the total surface subsidence within six months after mining less than 30 mm can be the symbol of surface stability and subsidence end (State Administration of Coal Industry 2017). In fact, the surface subsidence will continue to increase due to building loads which is defined as "additional subsidence" (Sun *et al.* 2015, Wang *et al.* 2015, Sasaoka *et al.* 2015, Ma *et al.* 2021). In general, additional subsidence has little effect on the small building facilities, but greater harm to large building facilities (Ma *et al.* 2021, Liu *et al.* 2017, Zhang *et al.* 2016, Zhu *et al.* 2014). On this basis, the stability of surface additional subsidence under building loads is important for the utilization of settled goafs.

To analyze the stability of settled goaf and determine the number of layers of buildings, it is necessary to judge whether the influence range of building load overlaps with the water-conducting fracture zone in goaf. The influence depth of building load is determined by the additional stress, namely the 10% of self weight stress. There are three situations between the influence depth of building load and the development height of the water-conducting fracture zone. When the influence depth enters the water-conducting fracture zone, the goaf stability can be affected by the building load, and the building will be affected by uneven settlement.

With full consideration of various factors, finite difference method simulation can quickly obtain the intuitive criterion of foundation stability (Ao *et al.* 2016, Wang *et al.* 2008, Xia *et al.* 2020, Li *et al.* 2022). Wang *et al.* (2019) simulated the ground disturbance laws of different building positions through FLAC3D. Wang *et al.* (2021a, b) carried out a lot of rock burst work by numerical simulation. Trueman (1990) derived the stress-strain

*Corresponding author, Ph.D.
E-mail: jiangning@sdust.edu.cn

ISSN: 2005-307X (Print), 2092-6219 (Online)

formula of longwall coal mining goaf material and used these datas in a finite element numerical model to investigate vertical stress build up in the waste. Zhang et al (2017) conducted a numerical model on the subsidence of longwall mining within continuum poromechanics and finite element setting and obtained the law of overlying strata deformation.

Gangue belongs to bulk media, and its gradation feature has a great influence on compression performance. Accurate acquisition of gradation characteristics of gangue is greatly significant to compression test simulation and gradation improvement design (Jiang *et al.* 2022, Lu *et al.* 2022). Experiments show that the deformation modulus of coal gangue samples with Talbot classification is higher than that of fully graded and single graded coal gangue samples. Hence, the characteristics of fractured rock mass in settled goaf after long time compression can be simulated (Li *et al.* 2016).

In this paper, take the goaf mined by two-layer coal mining as the engineering background, FLAC3D is adopted to simulate the surface movement and deformation law under different water-filling conditions. In order to obtain accurate bulk modulus and shear modulus of the water-conducting fracture zone in numerical simulation, the crushed gangues in the caving zone are taken from adjacent mine to conduct crushing gangue compression test under different water-bearing conditions. FISH language is used to perform gradient loading on the two-layer coal seams mining goaf and simulate the disturbance of the building load on the foundations. By monitoring, extracting and comparing the values of additional stress and self-weight stress of foundation under different building loads, the allowable applied load and ground disturbance depth of overlying strata foundation in goaf are obtained, which provides reference for practical engineering operation.

2. Engineering background

As shown in Fig. 1, the goaf of Shengjing Coal Mine is located in north of Jingshi Road and about 20 km north of Jiqing Expressway, Zhangqiu City, Shandong Province. A new E-commerce Industrial Park is planned to be distributed in the goaf of Shengjing Coal Mine. The Data Center is the core of the Shandong Lanhai pilot E-Commerce Industrial Park.

Most of the surface is covered by Quaternary sediments. According to the drilling data, the strata in the area from bottom to top are: Ordovician Majiagou Formation, Carboniferous-Permian Shanxi Formation, Taiyuan Formation, Benxi Formation, and Quaternary Dazhan Formation. Fig. 2 shows the main coal-bearing strata in Shengjing coal mine, namely Shanxi formation and Taiyuan formation.

Shanxi formation belongs to continental sedimentary facies, mainly sandstone, containing four coal seams. Among them, the upper No. 1,2,3 coal seams are unstable and unmined, No. 4 coal seam can be mined locally. Taiyuan formation belongs to marine and continental sedimentary facies. It contains 5 layers of limestone and 12 layers of coal.

Fig. 1 Location of ShengJing Mine

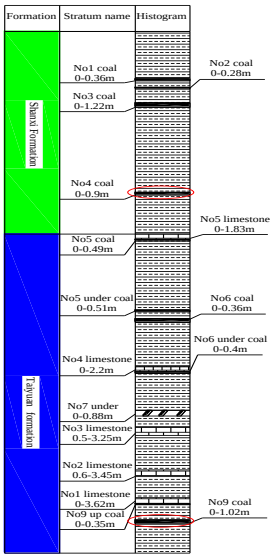

Fig. 2 Stratigraphic occurrences

The main minable coal seams were No. 4 and No. 9 coal seam. No. 4 adopted tunnel mining with about 50% recovery rate. The mining width was 5m. No. 9 coal seam adopted longwall mining with about 95% recovery rate. According to the data of construction borehole, the goaf of No.9 was soaked with water, while the goaf of No.4 was in the dry state. Table 1 shows the mining situation of each coal seam.

3 Theory analysis

3.1 Qualitative analysis of settled goaf activation in study area

As longwall mining advances, the overlying strata continues to crack with expansion of the goaf. These cracks develop downward and upward with intersection, forming a fracturing arch structure. Two kinds of space structure are formed by different mining scopes and lithology of

Table 1 Mining status of coal seams

Coal seams	Depth of cover/m	Average mining thickness/m	Coal-mining method	Coal-mining technology	Roof management	Recovery rate
No.4	38	0.67	Tunnel mining	Blasting mining	Caving method	50%
No.9	135	1.09	Longwall mining			95%

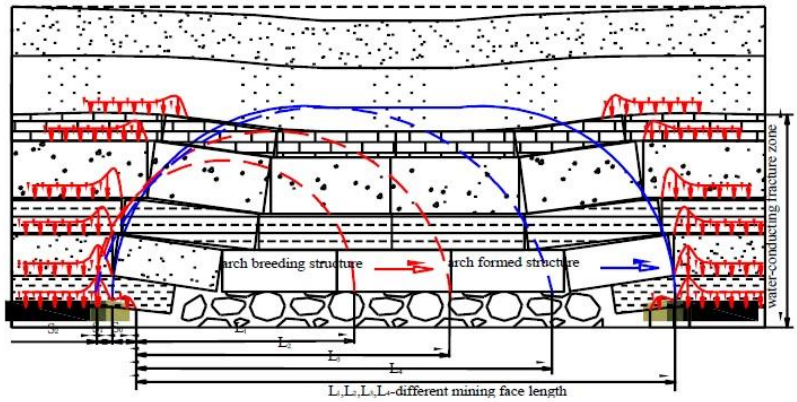

Fig. 3 Structural model evolution in longwall goaf of different mining state

overlying strata, namely the arch breeding structure and the arch formed structure, as shown in Fig. 3 (Rezaei *et al*. 2015, Jaouhar *et al*. 2018).

In the study area, No. 4 coal seam was operated privately by tunnel mining with irregular mining. Therefore, it was considered as incomplete mining state, the structural model of overlying strata in goaf was the arch breeding stage. The mechanical structure of stope can be regarded as a bending plate structure with a central suspension embedded in the surrounding coal body. No. 4 coal seam was the shallow seam, the bending structure of the plate tended to break and the goaf was easily activated under building or dynamic load.

Longwall mining was adopted in the No. 9 coal seam and could be seen as the complete mining state. The mechanical structure of stope was the bending plate structure which was embedded around the surrounding coal wall and overlapped on the central gangue of the goaf. The structure of overlying strata was the arch formed stage. There were several main causes for the activation of overlying strata, including the long-term slow compaction of broken gangue mass, sliding instability of rock beam in block articulated zone and rotation instability of rock beam, etc.

The results of borehole exploration show that there are many voids and fissures in the mining induced strata, which may lead to sudden collapse under the action of building loads. Drilling results show that 17 exploration drilling boreholes have been dropped in the goaf of No. 4 coal seam with a drop rate of 29%; 8 exploration drilling boreholes have been dropped in the goaf of No. 9 coal seam with a drop rate of 17%. It indicates that there are still some voids and fissures in the goaf of No. 4 and No. 9 coal seams. With the passage of time, this area will be subject to the subsidence and destruction under the influence of weathering, loading or earthquake.

3.2 Quantitative analysis of settled goaf activation in study area

Combined actual drilling conditions and empirical formula (State Administration of Coal Industry 2017), the heights of caving zone and water conducting fracture zone are 4 m and 13.4 m in No. 4 goaf, respectively. As to the No.9 goaf, there are 8 m and 29.6 m, respectively. According to the park building planning, the average load of building foundation is 1.1 MPa, the secondary activation of the settled No. 4 goaf can occur easily because of the shallow burial. According to the design plan, the pile-raft structure was adopted and the pile was driven to the goaf of No. 4 coal seam, as shown in Fig. 4.

Quaternary surface soil layer in this area is about 10 m, whose calculated bulk density is 15 kN/m^3, and the calculated bulk density of the following strata is 25 kN/m^3. Data Center is 84.84 m long in east and west, 59.64 m wide in north and south. The pile is end-bearing pile with diameter of 900 mm and 1000 mm and the spacing between piles is 8.4 m. Single pile capacity load is 1000 t, and there are 88 piles totally. The pile is designed to be driven to the floor of No. 4 coal seam.

According to the additional stress method and soil mechanics foundation, the gravity stress in foundation is calculated by the following formula

$$\sigma_c = r_1 h_1 + r_2 h_2 + \cdots + r_n h_n \quad (1)$$

Where r_1、r_2、$\cdots r_n$ is the bulk density of soil or rock from top to bottom layers in a foundation, kN/m^3; h_1、h_2, h_n is the thickness of soil or rock from top to bottom layers in a foundation, m.

The surface soil layer of Quaternary in this area is about 10 m, the calculated bulk density of the surface soil layer is

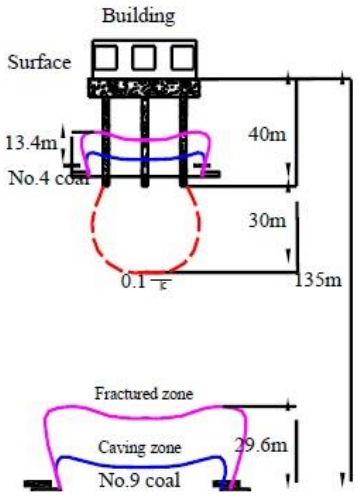

Fig. 4 Additional load influence depth of Data Center

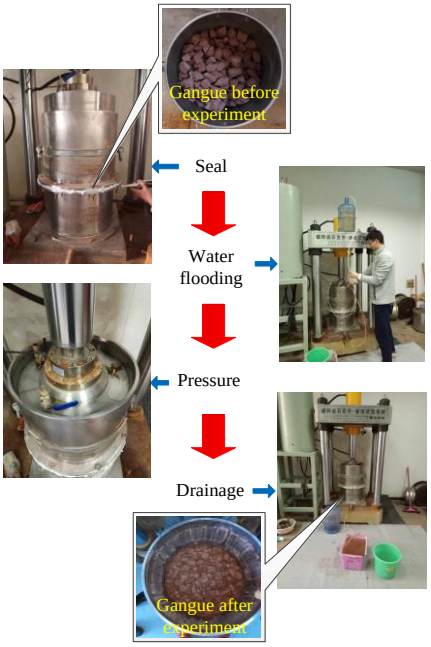

Fig. 5 Crushing gangue compression test in soaking state

15 kN / m^3, and the calculated bulk density of the rock below the surface soil layer is 25 kN / m^3.

According to the additional stress method and soil mechanics foundation, additional stress of the foundation is calculated by the following formula

$$\sigma_z = KP_0 \tag{2}$$

Where K is the Vertical additional stress coefficient under various loads (rectangular, square, bar loads, etc.).

P_0 is the average additional stress acting on foundation bottom, kN/m^2.

$$P_0 = P - r_0 D \tag{3}$$

Where P is the vertical uniform load on the foundation of residential building, kN/m^2. r_0 is the bulk density of natural soil above the foundation elevation, kN/m^3. D is the foundation depth, m.

According to the additional stress method, the additional stress of the local foundation is equal to 10% of the gravity stress of the foundation, which is the influence depth of the building load. The additional load influence depth of Data Center is 30.0 m under the base, as shown in Fig. 4.

According to the calculation results, there is a safe distance of 35.4 m between the additional load influence depth of Data Center and the water-conducting fracture zone in the goaf of No. 9 coal seam. The additional stress can not affect the water-conducting fracture zone of No.9 settled goaf.

While the goaf is likely to be reactivated according to the above qualitative analysis. It is necessary to study the influence of the building load to better protect the safety of the building.

4. Simulation analysis

The broken gangue basically recovers the approximate elastic state after a long time of compression, and according to the relevant references (Ao *et al.* 2016, Wang *et al.* 2008, Wang *et al.* 2019), FLAC3D is a general way to simulate the disturbance state of the settled goaf. Therefore, this paper uses FLAC3D to simulate the stability analysis of the settled goaf after the building load.

To accurately simulate the surface movement and deformation, the elastic modulus of rock mass with two fractured zones was obtained by crushing gangue compression test firstly, and deformation parameters in each zone were determined according to related referrences (Ao *et al.* 2016, Wang *et al.* 2008 Wang *et al.* 2019). Finally, to ensure the reliability of the simulation, the surface subsidence after normal mining was simulated and compared with the actual monitoring data.

4.1 Broken gangue compression test

As shown in Fig. 5, the deformation test system of broken gangue is mainly composed of main bearing support, test chamber and displacement stress double control servo system. The height of test chamber is 680 mm, the diameter of the test chamber is 400 mm, the maximum axial pressure can reach 600 kN. The maximum diameter of broken gangue is 60 mm according to the scale effect.

Gangue for testing were collected from adjacent mine to minimize experimental errors. Gangue were broken by a crusher, and sieved into 6 particle size ranges: 0~10 mm, 10~20 mm, 20~30 mm, 30~40 mm, 40~50 mm and 50~60 mm. In order to simulate the compression state of broken gangue in the old goaf, the broken gangue particle size distribution accords with Talbot grade n=0.4 distribution (Li *et al.* 2016), as shown in Table 3.

Linear loading was adopted in the broken gangue compression test. To simulate different buried depths, axial loads of broken gangue in No. 4 and No. 9 coal seams were increased by 0.5 kN/s axial loading rate to 188 kN or 440

Table 3 Particle size n=0.4 distribution

Particle size(mm)	0~10	10~20	20~30	30~40	40~50	50~60
Differential distribution(%)	0.08	1.15	5.02	13.50	28.47	51.78

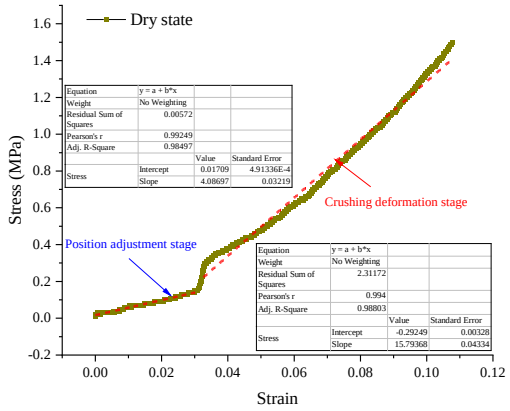

Fig. 6 Crushing gangue compression test in dry state of No. 4 coal seam

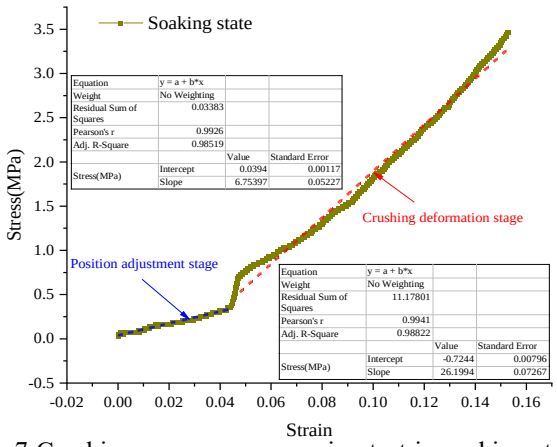

Fig. 7 Crushing gangue compression test in soaking state of No.9 coal seam

kN, namely 1.5 MPa or 3.5 MPa, respectively. Because the goaf of No. 4 and No. 9 coal seams were in the dry state and soaking condition, respectively. Therefore, the broken gangue compression test under dry state was conducted for goaf of No. 4 coal seam. While, broken gangue compression test under soaking state was conducted for No. 9 goaf only.

Fig. 5 shows the crushing gangue compression test in soaking state. The only difference in the crushing gangue compression test in dry state is that the water addition process is omitted.

4.2 Selection of rock mechanics parameters

As shown in Figs. 6 and 7, two deformation stages are involved in the stress-strain curve under the linear loading conditions, namely the position adjustment of the crushing rock in the initial stage and the crushing deformation in the later stage. The greater the stress, the greater the strain, namely the greater the burying depth, the more the deformation. broken gangue from No.9 coal seam is more fully compressed than that from No.4 coal.

The elastic modulus is obtained by Origin software fitting. The tangent compression modulus of No. 4 coal seam was 4.08 MPa under dry state in early deformation stage of position adjustment, changing to 15.79 MPa in later deformation stage. The tangent compression modulus of No.9 coal seam was 6.75 MPa under soaking state in early deformation stage, increasing to 26.20 MPa in later deformation stage.

To simulate the characteristics of broken gangue mass in the old goaf, the tangent modulus of the later stage was taken for the follow-up analysis. Based on the results of compaction test and related literature (Ao *et al*. 2016, Wang *et al*. 2008, Wang *et al*. 2019), the bulk modulus K, shear modulus G and other rock parameters of broken gangue were determined after reasonable simplification. Table 4 shows these parameters.

The model parameters for the remaining rock layers were selected from the uniaxial compressive and tensile strengths by indoor experiments based on cores drilled from the No.4 coal floor and below. The cohesion and friction angle were estimated by the program shear_strength_evaluate.exe prepared by Mr. Chong Shi of Hohai University.

Table 4 shows these parameters.

The simulated coal seams were No.4 coal and No.9 coal, whose buried depths were 38 m and 135 m respectively. A three-dimensional numerical model of FLAC3D which was 400 m long(X-axis), 300 m wide(Y-axis) and 160 m(Z-axis) high was established and divided into 20 layers from top to bottom, shown in Fig. 8(a). The working face was 160-meter-wide, advanced 300 m upward in the strike direction and leaving 100 m boundary pillar on the left side, that was the open-off cut side. The Mohr-Coulomb model was adopted in the simulation. Displacement boundary conditions were used except for the top boundary.

Figs. 8(b)-8(d) shows the vertical and horizontal displacement of the surface after normal mining. When the No.4 coal goaf was in the dry state, the No.9 coal goaf was in the soaking state, the maximum surface subsidence after mining was 399 mm, and the maximum value was above the central position of the goaf, as shown in Fig. 8(b). The maximum horizontal movement was 53.8 mm in the X direction, it was located at the intersection of the X=126 m and the measured line, as shown in Fig. 8(c). The maximum horizontal deformation in the Y direction was 6.02 mm, it was located at the intersection of the Y=80, Y=220 and X=400, as shown in Fig. 8(d). These data were basically consistent with the field monitoring results. The parameters of crushed gangues compression test and fracture zone could reflect the movement and deformation of overlying strata. It was reasonable to simulated disturbance laws of foundation under different building loads by FLAC3D.

Table 4 Rock mechanics parameters in numerical simulation

Rock stratum name	K (MPa)	G (MPa)	Cohesion (MPa)	Friction angle (°)	Tensile strength (MPa)	Density (kg/m^3)
Medium sandstone	2100	1260	2.23	50	3.71	2821
Siltstone	1230	690	3.72	46	2.65	2803
Mudstone	820	520	2.80	45	1.30	2630
No.9 coal seam	950	750	3.80	28	0.90	1400
Fine sandstone	890	750	3.40	32	1.46	2580
Limestone	690	430	3.38	39	1.68	2630
Clay	10	6	0.36	25	0.10	1800
No.9 coal caving zone （Soaking state）	7.28	5.46	0.042	15	0.002	1754
No.4 coal caving zone （Dry state）	4.68	3.51	0.042	18	0.002	1470
Fracture zone （Dry state）	1/10	1/10	1/2	Unchanged	1/2	Unchanged

Note: These parameters in the fracture zone affected by mining were correlation coefficients of mechanical parameters of the original rock mass

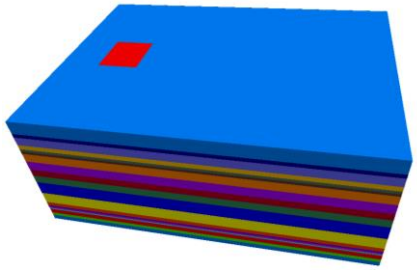

(a) Model grid diagram

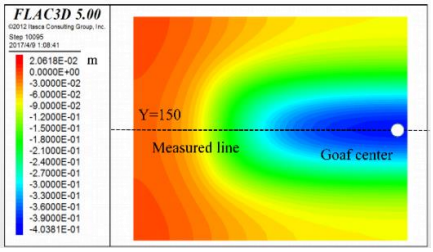

(b) Vertical displacement

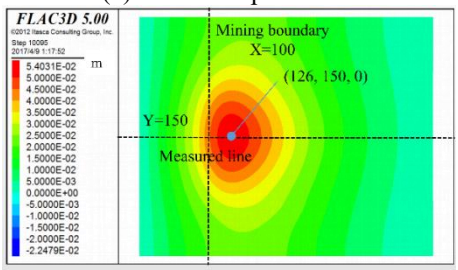

(c) X direction horizontal displacement

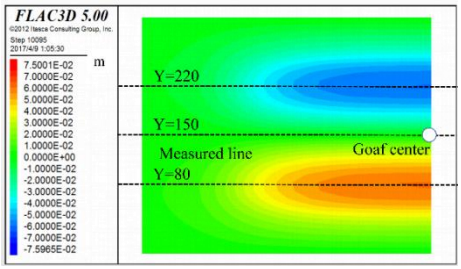

(d) Y direction horizontal displacement

Fig. 8 Displacement in different direction of surface

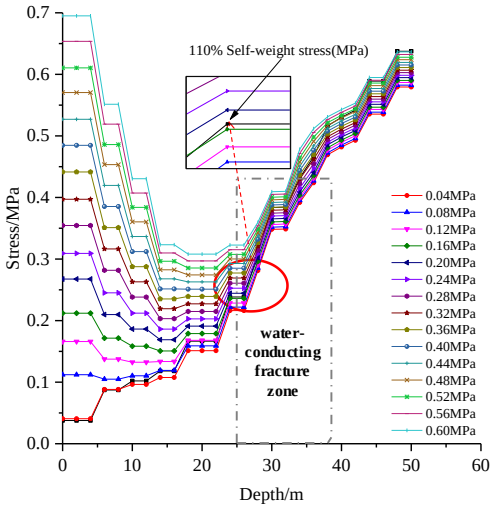

Fig. 9 No. 4 coal goaf stress propagate of different building loads

4.3 Disturbance law of overlay ground in No.4 coal goaf

Critical influence depth under critical building load is an important index to determine whether the settled goaf is "activated". FISH language was used to analyze the foundation individually to determine the maximum building load on the surface, the influence depth of building load on the foundation, and judge the stability of building foundation and the appropriate number of layers of buildings. The load was applied step by step, and the influence depth of building load was determined by the additional stress, namely the 10% of self weight stress.

No.4 coal goaf was close to the surface and could bear less building load without grouting treatment. The applied load gradient was 2 times the vertical uniform load of 20 kN/m^2 at the bottom of single-story residential building. The disturbance depth of overburden foundation in coal goaf is shown in Fig. 9.

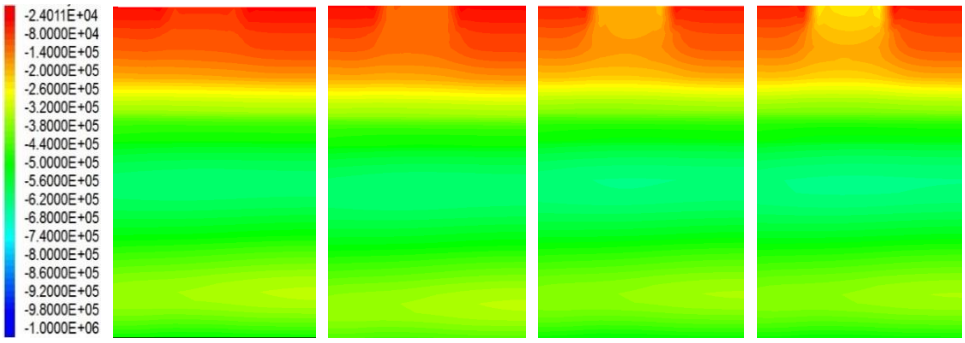

(a) 0.04 MPa (b) 0.08 MPa (c) 0.12 MPa (d) 0.16 MPa

Fig. 10 No. 4 coal goaf overburden additional stress propagation variation

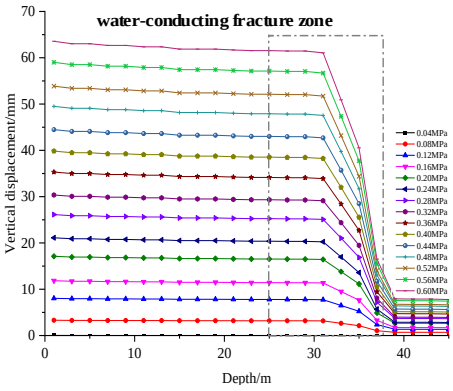

Fig. 11 No. 4 coal goaf overburden vertical deformation

4.3.1 Influence depth under different building loads

The results of numerical simulation and monitoring show that the allowable load was about 0.16 MPa and the influence depth was about 20 m. The maximum horizontal movement of foundation was 1.23 mm, the maximum vertical subsidence of foundation was 11.6 mm, and the safety distance between the influence range of additional stress of building load and the water-conducting fracture zone of coal goaf was about 5 m.

4.3.2 Additional stress under different building loads

Fig. 10 shows the change of additional stress propagation under the building loads of 0.04 MPa, 0.08 MPa, 0.12 MPa and 0.16 MPa at the section Y=150 m. When the applied load was 0.04 MPa, the stress propagation increased gradually from shallow to deep. When the applied load was 0.08 MPa, the stress value changed little, after the buried depth was more than 15 m, the stress increased gradually. When the applied load was greater than 0.08 MPa, the stress propagation decreased first and then increased.

4.3.3 Vertical deformation under different building loads

Fig. 11 shows the vertical deformation of overlying strata in No. 4 coal goaf. From the surface to the bent subsidence zone, the vertical displacement of the overburden increased linearly, and the displacement gradient increased sharply in the height range of the water conducting fracture zone, especially in the caving zone.

4.4 Disturbance law of overlay ground in No.9 coal goaf

According to the plan of the park, the average load of the building foundation was 1.1 MPa, which will influence the water conducting fracture zone in No. 4 settled goaf, so the reinforcement treatment for No.4 coal goaf was needed. According to the design planning foundation, the "pile+raft" structure is adopted, and the pile was designed to the No. 4 coal floor. The simulated load gradient was applied 5 times of the residential building vertical uniform load on the bottom of the foundation.

4.4.1 Influence depth under different building loads

Fig. 12(a) shows the influence depth of the overlying strata foundation in the goaf of No. 9 coal seam. The monitoring results indicated that 110% of the self weight stress was positively correlated with the depth. Under the action of building load, the vertical stress first decreased and then increased in the range of No. 4 and No. 9 coal seams. And with the increase of building load, this trend became more and more obvious.

In particularly, when the applied load changed from 1.5 MPa to 1.6 MPa, the vertical stress, that was the sum of origin stress and the additional stress in the water-conducting fracture zone exceeded 110% of self-weight stress. At this time, the influence range of additional stress of building load coincided with the water-conducting fracture zone in the goaf of No. 9 coal seam.

According to the monitoring results of Fig. 12(b), the influence depth of additional stress increased with the increase of building load, and the safety distance decreased. When the applied load was less than 0.9 MPa, the relationship between the influence depth and the applied load increases linearly. When the applied load was greater than 0.9 MPa, the relationship between the influence depth and the applied load increased nonlinearly, and the influence value of the unit load decreased gradually.

4.4.2 Additional stress under different building loads

Fig. 13 shows the change of additional stress propagation under the building loads of 0.5 MPa, 1.0 MPa, 1.5 MPa and 2.0 MPa at the section Y=150 m. When the building was applied, the stress propagation decreased first and then increased. Within the influence range of additional

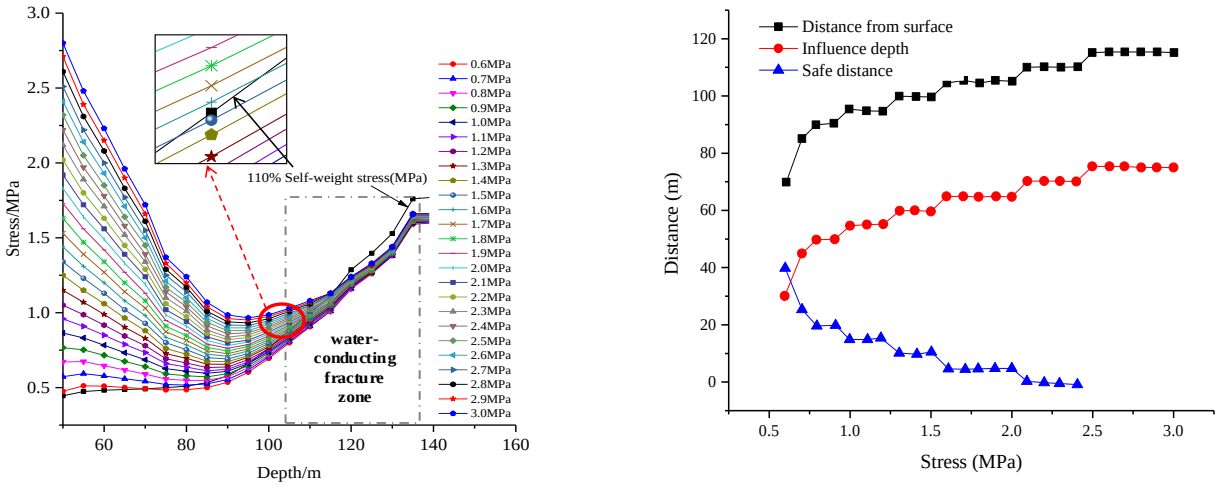

(a) (b)

Fig. 12 No. 9 coal seam stress propagate of different building loads and influence depth

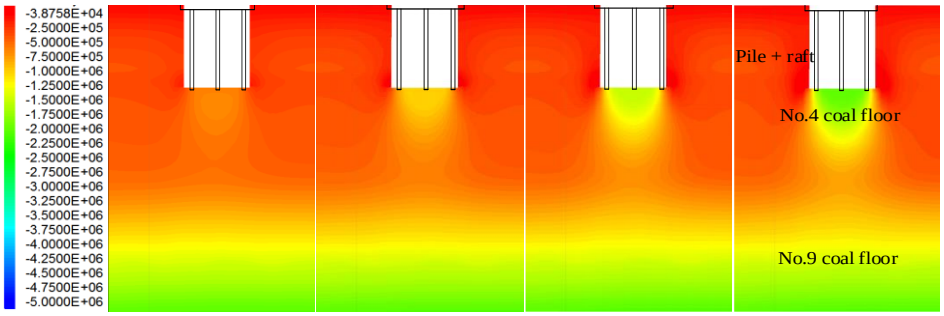

(a) 0.5 MPa (b) 1.0 MPa (c) 1.5 MPa (d) 2.0 MPa

Fig. 13 Additional stress propagation variation of overlying strata in No. 9 coal goaf

stress on foundation, the unit depth gradient value of additional stress increased gradually with the increase of applied stress.

The stress value curve was shaped as concave, the distribution pattern of additional stress has the following characteristics:

(1) Additional stresses were different on the same horizontal plane, the maximum was located on the central line and the values gradually decreased along both sides.

(2) At any point along the vertical direction under the load distribution, the additional stress decreased nonlinearly with the increase of foundation depth.

(3) If the point of additional stress was connected into a surface in space, the additional stress contour, the surface was shaped as a bubble.

4.4.3 Vertical deformation under different building loads

Fig. 14 shows the vertical deformation of overlying strata in No. 9 coal goaf. When the applied load was less than 0.9 MPa, the vertical deformation of overlying strata increased linearly, and the deformation gradient increased sharply within the influence range of caving zone. When the applied load was greater than 0.9 MPa, within the height range of the bending subsidence zone, vertical displacement gradient decreased with the increase of depth under fixed load. Within the height range of bending subsidence zone and caving zone, the vertical displacement gradient of overlying strata under the fixed load increased with the increase of depth, and the vertical displacement gradient of caving zone increased sharply within the influence range.

There was a greater vertical deformation from the loading position to the buried depth of 65 m. The deformation value and variation gradient increased with the increase of applied load, which was greatly affected by the additional stress. The deformation value tended to be stable and decreased gradually from the buried depth of 65 m ~ 110 m. The area with buried depth of 110 m to the goaf of No. 9 coal seam was the influence range of water-conducting fracture zone, and the deformation decreased sharply to a small deformation value.

As shown in Fig. 14, when the additional stress was less than 10% of the gravity stress in the central goaf, that is, the average load of the building foundation was less than 1.6MPa, the subsidence value of bending subsidence zone was more than that of water conduction fracture zone. It shows that the additional stress was too small and only had obvious effect on the deformation of shallow strata, that is, the deformation of the bending subsidence zone. When the additional stress was more than 10% of the gravity stress, that is, the average load of the building foundation was more than 1.6 MPa, the subsidence value of water-

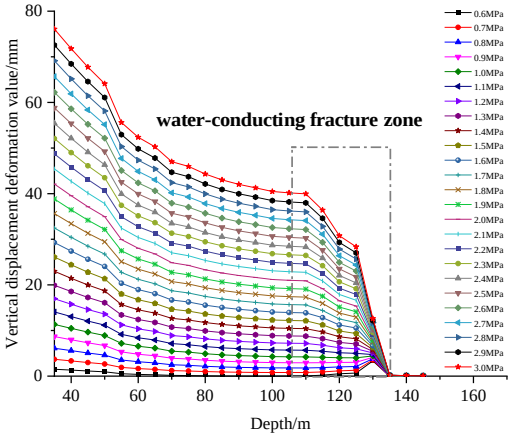

Fig. 14 Vertical deformation of overlying strata in the goaf of No. 9 coal seam

conducting fracture zone was more than that of bending subsidence zone. It shows that the additional stress had obviously affected the water-conducting fracture zone, superimposed the deformation of bending subsidence zone, and the deformation of overburden rock increased greatly.

5. Conclusions

Through the qualitative analysis of overburden strata failure mode, pre-geological exploration, borehole detection, there was a possibility of activation in the two-layer coal settled goaf, especially the No.4 settled goaf. Through the quantitative analysis of additional stress method, building load wouldn't influence the water-conducting fracture zone of No.9 settled goaf.

According to the compression test of broken gangue, the tangent compression modulus of No. 4 coal seam was 4.08 MPa under dry state in early deformation stage of position adjustment, changed to 15.79 MPa in later deformation stage. The tangent compression modulus of No.9 coal seam was 6.75 MPa under soaking state in early deformation stage, increased to 26.20 MPa in later deformation stage.

Under the action of building load, the vertical stress first decreased and then increased in the range of No. 4 and No. 9 coal seams. With the increase of building load, this trend became more and more obvious. The influence depth of additional stress increased with the increase of building load, and the safety distance decreased. With the increase of building load, this trend became step type.

When the building load was greater than 0.16 MPa, the water-conducting fracture zone of No.4 goaf would be influenced. When the building load was greater than 1.6 MPa, the additional stress affected the water-conducting fracture zone of No.9 goaf. The subsidence value of water-conducting fracture zone was greater than that of bending subsidence zone.

Data availability statement:

All the data in this paper are available.

Funding

This paper is supported by Anhui Provincial Key Research and Development Project (2022m07020006), Anhui Provincial Natural Science Foundation (2208085ME124), Shandong Provincial Natural Science Foundation (ZR2020QE102 , ZR2019BEE013); SDUST Research Fund (2019TDJH101); Shandong postgraduate education quality improvement plan project (No. SDYJG19062); Research project of undergraduate teaching reform in Shandong Province (No. P2020013); National Natural Science Foundation of China (52004146,51974178, 52074169, 52174159); China Postdoctoral Science Foundation (2022M713386) ; the Research Fund of Key Laboratory of Deep Coal Resource Mining (CUMT), Ministry of Education (KLDCRM202102) and the 2020 Joint Fund for the Project of the State Key Laboratory of Coal Resources and Safe Mining-Outstanding Young Scientists Program of Beijing Higher Education Institutions (SKLCRSM20LH04).

Conflicts of Interest

The authors declare no conflict of interest.

References

Ao, X., Wang, X., Zhu, X., Zhou, Z. and Zhang, X. (2016), "Grouting simulation and stability analysis of coal mine goaf considering hydromechanical coupling", *J Comput Civ Eng*., **31**, 04016069. https://doi.org/0.1061/(ASCE)CP.19435487.0000640.

Jaouhar, E.M., Li, L. and Aubertin, M. (2018), "An analytical solution for estimating the stresses in vertical backfilled stopes based on a circular arc distribution", *Geomech. Geoeng*., **15**(3), 889-898. https://doi.org/10.12989/gae.2018.15.3.889.

Jiang, N., Wang, C.X., Pan, H.Y., Yin, D.W. and Ma, J.B. (2020), "Modeling study on the influence of the strip filling mining sequence on mining-induced failure", *Energy Sci Eng*., **8**, 2239-2255. https://doi.org/10.1002/ese3.660.

Jiang, N., Yin, D., Ma, J., Han, L. and Yin, Q. (2021), "Effects of water immersion on the long-term bearing characteristics of crushed gangue in goaf", *Geofluids*., **2021**(1), 1-11. https://doi.org/10.1155/2021/6675984.

Jiang, N., Lv, K., Gao, Z., Di, H., Ma, J. and Pan, T. (2022), "Study on characteristics of overburden strata structure above abandoned gob of shallow seams—A case study", *Energies*, **15**(24), 9359. https://doi.org/10.3390/en15249359.

Karabork, T., Bilgehan, R.P. and Deneme, I.O. (2014), "A comparison of the effect of SSI on base isolation systems and fixed-base structures for soft soil", *Geomech. Eng*., **7**(1), 87-103. https://doi.org/10.12989/gae.2014.7.1.087.

Li, F.X., Yin, D.W., Wang, F., Jiang, N. and Li, X.L. (2022), "Effects of combination mode on mechanical properties of bi-material samples consisting of rock and coal", *J Mater. Res. Technol*., **19**, 2156-2170. https://doi.org/10.1016/j.jmrt.2022.05.174.

Li, M., Zhang, J. and Gao, R. (2016), "Compression characteristics of solid wastes as backfill materials", *Adv Mater Sci Eng*., **2016**. https://doi.org/10.1155/2016/2496194.

Liu, H., Deng, K., Lei, S., Bian, Z. and Chen, D. (2017), "Dynamic developing law and governance standard of ground fissures caused by underground mining", *J Min Saf Eng*., **5**, 884-890. https://doi.org/10.13545/j.cnki.jmse.2017.05.009.

Lu, Y., Jiang, N., Lu, W., Zhang, M., Kong, D., Xu, M. and Wang, C. (2022), "Experimental study on deformation characteristics of gangue backfill zone under the condition of natural water in deep mines", *Sustainability*, **14**, 15517. https://doi.org/10.3390/su142315517

Ma, J., Jiang, N., Wang, X., Jia, X. and Yao, D. (2021), "Numerical study of the strength and characteristics of sandstone samples with combined double hole and double fissure defects", *Sustainability-Basel*., **13**(13). https://doi.org/10.3390/su13137090.

Pan, H., Jiang, N., Gao, Z., Liang, X. and Yin, D. (2022), "Simulation study on the mechanical properties and failure characteristics of rocks with double holes and fractures", *Geomech. Eng*., **30**(1), 93-105. https://doi.org/10.12989/gae.2022.30.1.093.

Rezaei, M., Hossaini, M.F. and Majdi, A. (2015), "A time-independent energy model to determine the height of destressed zone above the mined panel in longwall coal mining", *Tunn. Undergr. Sp. Tech.*, **47**, 81-92. https://doi.org/10.1016/j.tust.2015.01.001.

Sasaoka, T., Takamoto, H., Shimada, H., Oya, J., Hamanaka, A. and Matsui, K. (2015), "Surface subsidence due to underground mining operation under weak geological condition in Indonesia", *J. Rock Mech. Geotech. Eng*., **7**, 337-344. https://doi.org/10.1016/j.jrmge.2015.01.007.

Soomro, M.A., Mangi, N., Memon, A.H. and Mangnejo, D.A. (2022), "Responses of high-rise building resting on piled raft to adjacent tunnel at different depths relative to piles", *Geomech. Eng*., **29**(1), 25-40. https://doi.org/10.12989/gae.2022.29.1.025.

State Administration of Coal Industry (2017), "Regulations for the preservation and mining of coal pillars in buildings, water bodies, railways and main roadways", Coal Industry Publishing House: Beijing, China.

Sun, Y., Zhang, X., Mao, W. and Xu, L. (2015), "Mechanism and stability evaluation of goaf ground subsidence in the third mining area in Gong Changling District, China", *Arabian J. Geosci*., **8**, 639-646. https://doi.org/10.1007/s12517-014-1270-9.

Tan, Y., Xu, H., Yan, W.T., Guo, W.B., Bai, E.H., Qi, T.Y., Yin, D.W., Hao, B.Y., Cheng, H. and Shao, M.H. (2022), "Study on the overburden failure law of high-intensity mining in gully areas with exposed bedrock", *Front Earth Sc-Switz*., **10**, 833384. https://doi.org/10.3389/feart.2022.833384.

Tan, Y., Xu, H., Yan, W.T., Guo, W.B., Sun, Q., Yin, D.W., Zhang, Y.J., Zhang, X.Q., Jing, X.F., Wei. S.J. and Liu, X. (2022), "Development law of water conducting fracture zone in the fully mechanized caving face of gob-side entry driving: A case study", *Minerals-Basel*, **12**, 557. https://doi.org/10.3390/ min12050557.

Toprak, B., Bas, S. and Kalkan, I. (2021), "Effects of fly ash column treatment of HP clayey soils on seismic behavior of R/C structures", *Geomech. Eng*., **25**(6), 473-480. https://doi.org/10.12989/gae.2021.25.6.473.

Trueman, R. (1990), "A finite element analysis for the establishment of st ress development in a coal mine caved waste", *Int. J. Min. Sci. Technol*., **10**(3), 247-252. https://doi.org/10.1016/0167-9031(90)90452-X.

Wang, C.X., Lu, Y., Li, Y.Y., Zhang, B.C. and Liang, Y.B. (2019), "Deformation process and prediction of filling gangue: A case study in China", *Geomech. Eng*., **18**(4), 417-426. https://doi.org/10.12989/gae.2019.18.4.417.

Wang, C.X., Lu, Y., Qin, C.R., Li, Y.Y., Sun, Q.C. and Wang, D.J. (2019), "Ground disturbance of different building locations in old goaf area: A case study in China", *Geo. Geo. Eng*., **37**(5), 4311-4325. https://doi.org/10.1007/s10706-019-00909-x.

Wang, F., Zhang, C., Zhang, X. and Song, Q. (2015), "Overlying strata movement rules and safety mining technology for the shallow depth seam proximity beneath a room mining goaf", *Int. J. Min. Sci. Technol*., **25**, 139-143. https://doi.org/CNKI:SUN:ZHKD.0.2015-01-021.

Wang, J., Apel, D.B., Dyczko, A., Walentek, A., Prusek, S., Xu, H. and Wei, C. (2021), "Investigation of the rockburst mechanism of driving roadways in close-distance coal seam mining using numerical modeling method", *Mining, Metallurgy & Exploration*, **38**(5), 1899-1921.

Wang, J., Apel, D.B., Pu, Y., Hall, R., Wei, C. and Sepehri, M. (2021), "Numerical modeling for rockbursts: A state-of-the-art review", *J. Rock Mech. Geotech. Eng*., **13**(2), 457-478.

Wang, J., Ding, C., Zhang, Y. and Wu, S. (2008), "Numerical analysis of effect of abandoned goaf foundation deformation on ground buildings", *J Min Saf Eng*., **25**, 476-480. https://doi.org/10.3969/j.issn.1673-3363.2008.04.021.

Xia, Z., Jiang, N., Yang, H., Han, L. and Feng, Q. (2020), "Effect of multiple hole distribution and shape based on particle flow on rocklike failure characteristics and mechanical behavior", *Adv Civ. Eng*., **2020**(6), 1-13. https://doi.org/10.1155/2020/8822225.

Yao, D.H., Jiang, N., Wang, X.J., Jia, X. and Lv, K. (2022), "Mechanical behaviour and failure characteristics of rocks with composite defects of different angle fissures around hole", *B Eng. Geol. Environ.*, **81**(7). https://doi.org/10.1007/s10064-022-02783-z.

Zhang, B., Zhang, L., Yang, H., Zhang, Z. and Tao, J. (2016), "Subsidence prediction and susceptibility zonation for collapse above goaf with thick alluvial cover: a case study of the Yongcheng coalfield, Henan Province, China", *Bull. Eng. Geol. Environ*., **75**, 1117-1132. https://doi.org/10.1007/s10064-015-0834-6.

Zhang, X., Yu, H., Dong, J., Liu, S., Huang, Z., Wang, J. and Wong, H. (2017), "A physical and numerical model-based research on the subsidence features of overlying strata caused by coal mining in Henan, China", *Environ Earth Sci*., **76**, 705. https://doi.org/10.1007/s12665-017-6979-9.

Zhu, G., Xu, Z., Xie, C. and Guo, Y. (2014), "Study of influence functions of surface residual movement and deformation above old goaf", *China J. Rock Mech. Geotech. Eng*., **10**, 962-1970. https://doi.org/10.13722/j.cnki.jrme.2014.10.003.

IC